(2)

SEC

# AD-A204 972

REPORT DOCUMENTATION PAGE

Form Approved OMB No. 0704-0188

DTIC FILE COPY

| | |
|---|---|
| 1a. REPORT SECURITY CLASSIFICATION: Unclassified | 1b. RESTRICTIVE MARKINGS |
| 2a. SECURITY CLASSIFICATION AUTHORITY | 3. DISTRIBUTION/AVAILABILITY OF REPORT: Distribution Unlimited; approved for public release. |
| 2b. DECLASSIFICATION/DOWNGRADING SCHEDULE | |
| 4. PERFORMING ORGANIZATION REPORT NUMBER(S): JA 321:047:87 | 5. MONITORING ORGANIZATION REPORT NUMBER(S) |
| 6a. NAME OF PERFORMING ORGANIZATION: Physical Oceanography | 6b. OFFICE SYMBOL (If applicable) |
| 7a. NAME OF MONITORING ORGANIZATION: Naval Ocean Research and Development Activity | |
| 6c. ADDRESS (City, State, and ZIP Code) | 7b. ADDRESS (City, State, and ZIP Code): Stennis Space Center, MS 39529 |
| 8a. NAME OF FUNDING/SPONSORING ORGANIZATION: Office of Naval Research | 8b. OFFICE SYMBOL (If applicable): 321 |
| 9. PROCUREMENT INSTRUMENT IDENTIFICATION NUMBER | |
| 8c. ADDRESS (City, State, and ZIP Code): Arlington, VA | 10. SOURCE OF FUNDING NUMBERS |

| PROGRAM ELEMENT NO. | PROJECT NO. | TASK NO. | WORK UNIT ACCESSION NO. |
|---|---|---|---|
| W1AE | 2211 | 111 | 13217A |
| W1AE | 3205 | 330 | 13218A |

11. TITLE (Include Security Classification)
A Study of an Intense Density Front in the Eastern Alboran Sea: The Almeria-Oran Front

12. PERSONAL AUTHOR(S)
J. Tintore*, P.E. La Violette, I. Blade and A. Cruzado

| 13a. TYPE OF REPORT | 13b. TIME COVERED | 14. DATE OF REPORT (Year, Month, Day) | 15. PAGE COUNT |
|---|---|---|---|
| Journal Article | FROM ______ TO ______ | 1988 | 16 |

16. SUPPLEMENTARY NOTATION

| 17. COSATI CODES | | | 18. SUBJECT TERMS (Continue on reverse if necessary and identify by block number) |
|---|---|---|---|
| FIELD | GROUP | SUB-GROUP | Ocean fronts, remote sensing |
| | | | Mediterranean Oceanography |
| | | | Ocean Circulation |

19. ABSTRACT (Continue on reverse if necessary and identify by block number)


Studies of satellite imagery and space shuttle photographs of the western Mediterranean have indicated that the main path of inflowing Atlantic Water is around two large anticyclonic gyres in the Alboran Sea and along the Algerian Coast. These studies have also shown that a strong ocean front is present between Almeria, Spain, and Oran, Algeria, which is part of the easternmost segment of the Eastern Alboran Gyre. Based on these satellite studies, the first in situ investigation of the front, called here the Almeria-Oran Front, was conducted in March 1986 as part of the winter campaign of the Western




| | | |
|---|---|---|
| 20. DISTRIBUTION/AVAILABILITY OF ABSTRACT: ☐ UNCLASSIFIED/UNLIMITED ☐ SAME AS RPT. ☐ DTIC USERS | 21. ABSTRACT SECURITY CLASSIFICATION: Unclassified | |
| 22a. NAME OF RESPONSIBLE INDIVIDUAL: P. La Violette | 22b. TELEPHONE (Include Area Code): (601)688-4867 | 22c. OFFICE SYMBOL: 321 |

DD Form 1473, JUN 86 Previous editions are obsolete.

SECURITY CLASSIFICATION OF THIS PAGE

Unclassified

Unclassified

19. Abstract (Continuation)

Mediterranean Circulation Experiment (WMCE). Analyses of the resulting data show that the Almeria-Oran Front is a large-scale density front, formed by the convergence of two distinct water masses and controlled by geographic position and strength of the Eastern Alboran Gyre. Physical and biochemical data indicate that the front is limited to the upper 300 m, with a strong southward baroclinic jet. The secondary ageostrophic circulation is characterized by surface convergence, along isopycnal sinking, and upwelling on the western side of the front. (FR)

mJ

Reprinted from JOURNAL OF PHYSICAL OCEANOGRAPHY, Vol. 18, No. 10, October 1988
American Meteorological Society

# A Study of an Intense Density Front in the Eastern Alboran Sea: The Almeria–Oran Front

J. TINTORE

P. E. LA VIOLETTE

I. BLADE

A. CRUZADO

# A Study of an Intense Density Front in the Eastern Alboran Sea: The Almeria–Oran Front

J. TINTORE

*Dept. Fisica, Universitat de les Illes Balears, Palma de Mallorca, Spain*

P. E. LA VIOLETTE

*Naval Ocean Research and Development Activity, Stennis Space Center, Mississippi*

I. BLADE*

*Dept. Fisica, Universitat de les Illes Balears, Palma de Mallorca, Spain*

A. CRUZADO

*Centre d'Estudis Avancats de Blanes, CSIS, Cami Sta Barbara, Blanes, Gerona, Spain*

(Manuscript received 5 October 1987, in final form 5 April 1988)

ABSTRACT

Studies of satellite imagery and space shuttle photographs of the western Mediterranean have indicated that the main path of inflowing Atlantic Water is around two large anticyclonic gyres in the Alboran Sea and along the Algerian Coast. These studies have also shown that a strong ocean front is present between Almeria, Spain, and Oran, Algeria, which is part of the easternmost segment of the Eastern Alboran Gyre. Based on these satellite studies, the first in situ investigation of the front, called here the Almeria–Oran Front, was conducted in March 1986 as part of the winter campaign of the Western Mediterranean Circulation Experiment (WMCE). Analyses of the resulting data show that the Almeria–Oran Front is a large-scale density front, formed by the convergence of two distinct water masses and controlled by the geographic position and strength of the Eastern Alboran Gyre. Physical and biochemical data indicate that the front is limited to the upper 300 m, with a strong southward baroclinic jet. The secondary ageostrophic circulation is characterized by surface convergence, along-isopycnal sinking, and upwelling on the western side of the front.

## 1. Introduction

The Mediterranean Sea is an evaporative, semi-enclosed sea whose only substantial connection to the world ocean is the Strait of Gibraltar. Atlantic Water (AW) flowing through the Strait into the Mediterranean Sea at the surface overrides a deeper layer of dense Mediterranean waters outpouring into the Atlantic. The surface AW flow replaces both water evaporated within the sea and the subsurface outflow of Mediterranean waters.

The two basins of the Alboran Sea are the first Mediterranean basins encountered by the replacement AW. Thus, the Alboran acts as a transition area, since most of the mixing of the fresher AW with the highly saline Mediterranean waters occurs in these basins (e.g., Lanoix 1974; Lacombe and Tchernia 1972; Gascard and Richez 1985; Parrilla et al. 1986). The incoming AW salinity varies during its eastward migration through the Alboran—from 36.2 to 36.5 psu (practical salinity units)—being chiefly modified by upwelled Levantine Intermediate Water (LIW) and AW previously made more saline. The Modified AW (MAW), which forms the upper layer of the sea, ranges from 150 to 200 m in the center of the basins to 50 m near the Spanish coast. LIW, characterized by both temperature and salinity maxima, is generally found between 200 and 600 m, while Mediterranean Deep Water (MDW) with lower temperature and salinity is found below the MAW and LIW.

Although the regional circulation is mostly salinity driven, proper interpretation of satellite thermal imagery may be used to indicate the eastward path of the MAW (La Violette 1984; Arnone and La Violette 1986). This imagery indicates that the mean surface flow pattern in the Alboran Sea is composed of two adjacent anticyclonic gyres (called the Western and Eastern Alboran Gyres) that in their mean position overlay the two basins (Fig. 1).

* Present affiliation: Dept. of Atmospheric Sciences, University of Washington, Seattle, Washington.

*Corresponding author address:* Dr. Joaquin Tintore, Dept. Fisica, Universitat de les Illes Balears, Palma de Mallorca, Spain.

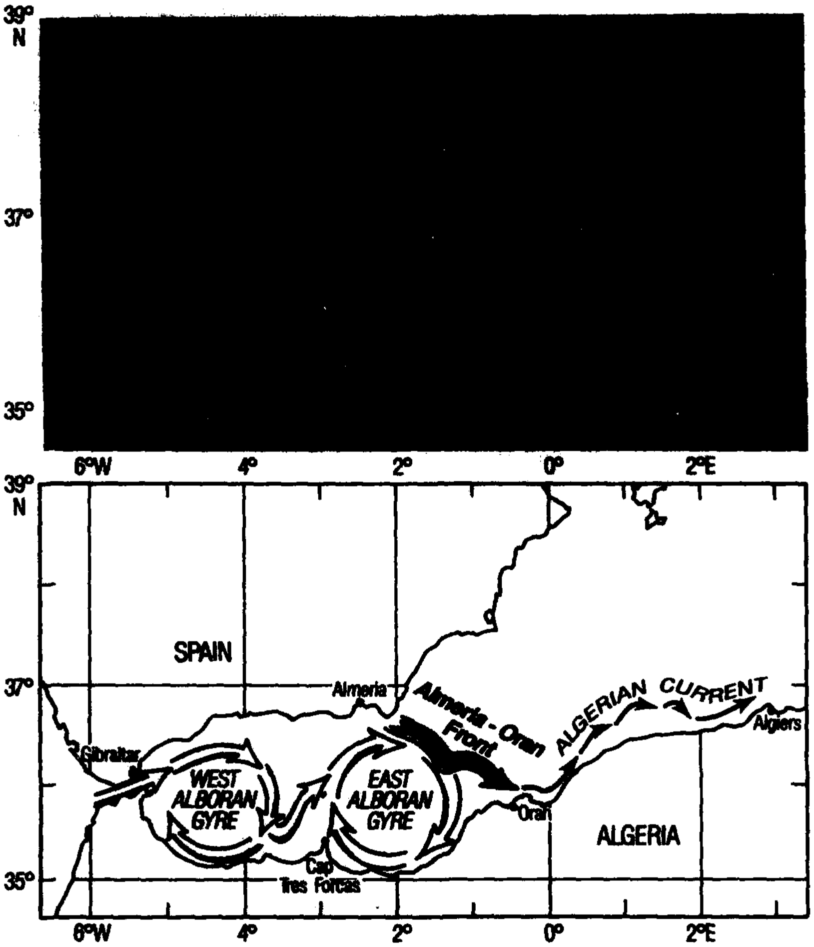


FIG. 1. (Top) A satellite thermal image of the Alboran Sea, showing the continuity of the regional circulation. As with the other satellite imagery in this paper, this NOAA AVHRR-IR image was registered to a Mercator projection and enhanced to show the ocean features. (Bottom) A schematic drawing of the circulation identifying the features displayed in the satellite thermal image (after Arnone et al. 1988).

Short-term (three to four week) pattern variations do occur, which vary substantially from the long-term mean position of the two gyres. On occasion, one or the other gyre may collapse (Figs. 2a, b) (Perkins et al. 1987; Heburn and La Violette 1987). Numerical models used to study the dynamics of the western Mediterranean Sea under the influence of various forcing mechanisms, i.e., winds, inflow/outflow through the straits, and buoyancy, indicate that the cause may be variations in the subsurface flow of MAW (Heburn and La Violette 1987; Werner et al. 1988).

Studies of the satellite imagery indicate that beyond the Alboran Sea, the mean flow of MAW continues eastward along the coast of Algeria until approximately 5°E, where its path is not as well defined. It appears that the variations in the structure of the Eastern Alboran Gyre and the orientation of the flow along the Algerian Coast are coupled (Heburn and La Violette 1987). Thus, understanding the processes that take place in the Eastern Alboran Gyre is an important step toward understanding one of the major circulation elements in the western Mediterranean Sea.

Satellite imagery indicates that part of the MAW flows close to the south Spanish coast until it reaches Cape Gata, and that east of the cape, resident Mediterranean water flows southwest along the eastern Spanish coast. Therefore, near Cape Gata there is a convergence of these two distinct waters, and the MAW is deflected southward toward Oran on the Algerian Coast. Near the coast, some of the MAW is retained within the anticyclonic circulation of the gyre, while the remainder continues eastward to form the Algerian

FIG. 2a. A NOAA-7 AVHRR-IR image of Alboran Sea showing only one anticyclonic gyre; the Western Alboran Gyre. This single gyre situation gradually changed over a four-week period to two full gyres as in Fig. 1 (Heburn and La Violette 1988).

Current. The result is that the eastern edge of the Eastern Gyre forms a well-defined frontal zone that can be seen in most of the satellite imagery. This intense permanent front, called here the Almeria–Oran Front, is the principal focus of this paper.

Although the Almeria–Oran Front has been noticeable in regional studies of satellite infrared imagery for several years (e.g., Philippe and Harang 1982; *Satmer*, any issue from 1983 on), no detailed in situ investigation had been made prior to the oceanographic cruise discussed here. Indeed, previous Alboran Sea studies do not indicate a front (e.g., Lanoix 1974; Cheney 1977), nor have earlier numerical models included this feature (e.g., Preller and Hulbert 1982). If anything, these studies reveal a cyclonic circulation in the eastern Alboran basin (Fig. 2). Did these early field efforts show the normal or anomalous conditions of the gyre? If they were anomalous what are "normal" conditions? One of the aims of the Western Mediterranean Circulation Experiment (WMCE) (La Violette 1987) is to investigate these questions, and a series of in situ investigations has been initiated.

In this paper, we present the results of a field investigation of the Almeria–Oran Front, which was conducted as part of the 1986 winter campaign of the WMCE. Because this is the first intensive field study of the front, it was planned as an exploratory investigation of the dynamics of the front. As a result, this report reflects the preliminary nature of the WMCE investigation. We first present a surface description of the front from satellite images and space shuttle photographs (section 2); we then combine the analyses of the physical, chemical, and biological data of the field investigation to define the main physical characteristics of this density front (section 3); and finally, we discuss frontal structure and induced circulation, and then develop a simple dynamical explanation of the front (section 4).

## 2. The satellite imagery and space shuttle photographs

In preparation for the WMCE studies of the Almeria–Oran Front, a brief field study was conducted in October 1984 using infrared satellite imagery, an aircraft and the U.S. space shuttle (Mission STS-41-G). Working in unison with the shuttle crew, the aircraft scientists made flights over the area, dropping airborne expendable bathythermographs (XBTs) to obtain vertical temperature sections of the front that were concurrent with the shuttle photographs and satellite infrared imagery.

Figure 3a is a mosaic made from 3 of the more than 15 shuttle photographs taken of the area. The geographic location of the mosaic in relation to the front is shown by the NOAA infrared image included in the figure. The shuttle photographs show the sun's reflection off the roughened sea surface. Since, in addition to wind stress and air–sea temperature differences, the sea's roughness varies with vertical and horizontal water movement, surface roughness patterns can delineate ocean events involving circulation. The roughness pattern displayed in the mosaic is partially a direct result of the vertical and horizontal circulation of the Almeria–Oran Front. (The prominent east–west lines in the photographs are ship tracks. Their displacement across the front provides a qualitative indication of the current shear.)

The aircraft infrared thermal scanner (uncalibrated) and search radar showed manifestations of the front that coincided with the features displayed in the mosaic. Most importantly, the airborne XBTs showed a temperature contrast of approximately 2°C across the front, and a deepening and weakening of the thermocline on its western side. Thus, they provided proof that the photographic and infrared displays of the Almeria–Oran Front revealed not just surface phenomena but subsurface structure.

Based on the results of the space shuttle/aircraft survey and persistence of the feature in the satellite imagery, the oceanographic cruise discussed in the next section was planned and conducted.

## 3. The oceanographic cruise

### *a. Data*

From 11 to 15 March 1986, a field study of the Almeria–Oran Front was conducted from the R/V *Garcia del Cid*. The objective was to study the structure of the front using continuous recorded surface temperature in combination with XBTs, conductivity–tempera-

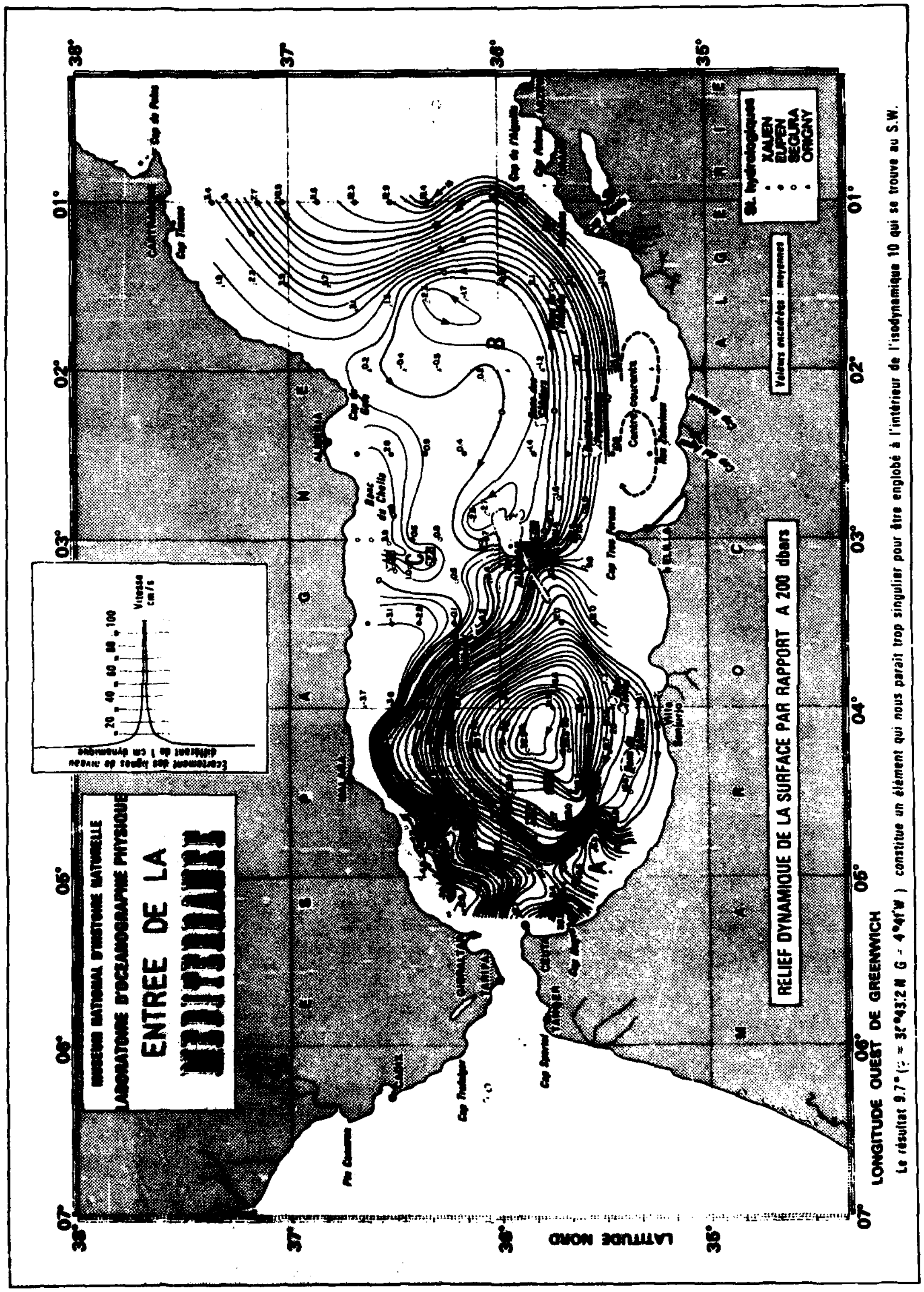


FIG. 2b. An analysis of ship data by Lanoix (1974) showing a situation similar to the satellite image in Fig. 2a.

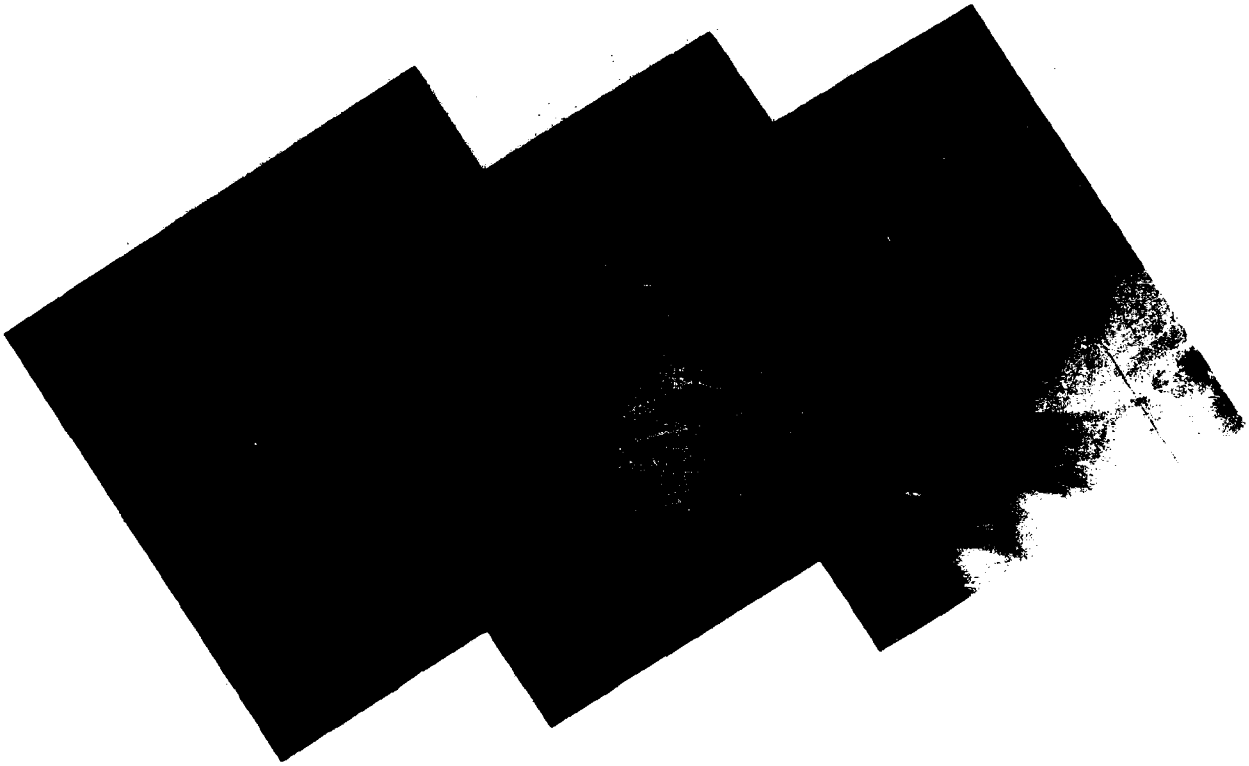

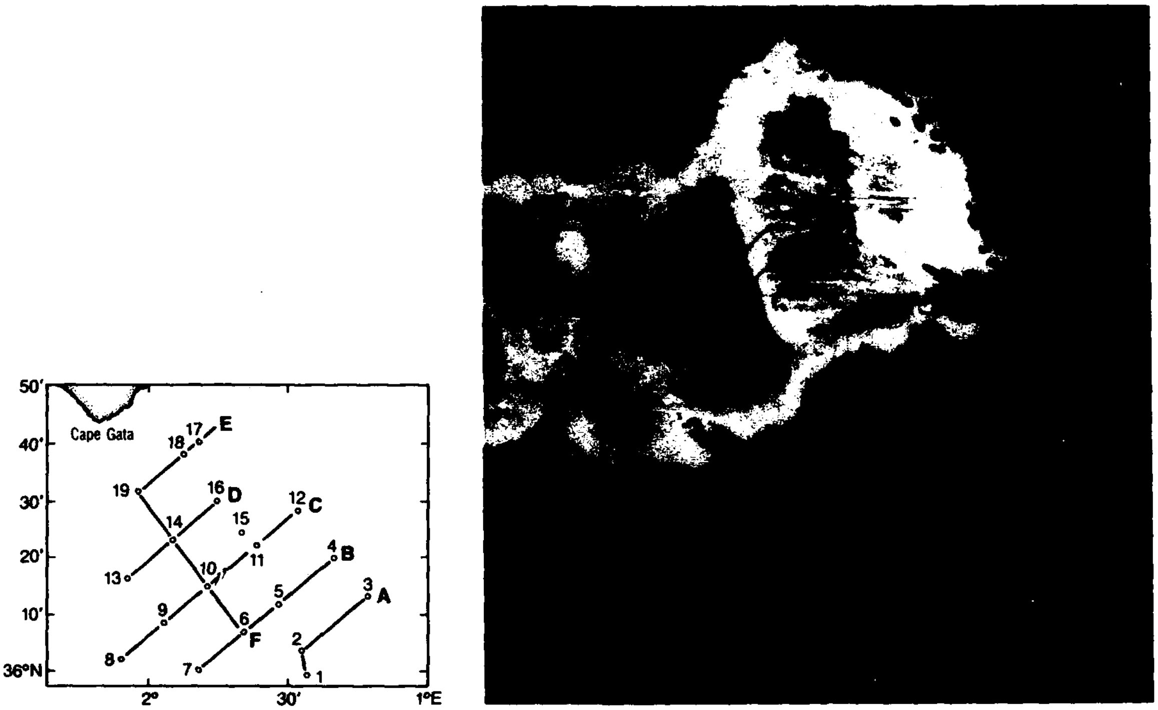


FIG. 4. (a) The 11-15 March cruise track of the R/V *Garcia del Cid* and position of the ocean stations. Note that the track was interrupted at Station 10 for 36 hours due to a storm. (b) Location of the cruise track in relation to the front as defined by a NOAA AVHRR-IR image for 14 March.

ture-depth (CTD) casts, and vertical sampling of salinity, nitrates, oxygen and chlorophyll. A last-minute breakdown of the CTD forced reliance on XBTs and hydrographic casts for the vertical sampling. As a result, the station spacing is much coarser than originally planned. Niskin bottles were placed at the standard depth levels: 0, 10, 20, 30, 50, 75, 100, 150, 200, 250, 300, 400 and 500 m. Spatial surface continuity was maintained using surface temperature, salinity and nitrate continuous recorders.

Surface temperatures and salinities were monitored with a Grundy MK2 thermosalinograph. Bottle salinities were measured using a Beckman induction salinometer. Nitrates were analyzed with a Technicon Auto-Analyzer following the method described by Strickland and Parsons (1972). Oxygen concentrations were obtained using the Winkler method described by Strickland and Parsons (1972) and chlorophyll concentrations by the technique of Jeffrey and Humphrey (1975).

Ship positions were obtained using satellite navigation. The cruise track and station locations are shown in Fig. 4a. The cruise was interrupted after Station 10 due to a strong westerly wind (20 m $s^{-1}$) and was re-

FIG. 3. (a) A mosaic of three photographs taken within seconds of one another from aboard U.S. Space Shuttle Mission STS-41-G near local noon on 8 October 1984 from an altitude of approximately 200 km (NASA photographs 38-079, 38-080, and 38-082. NASA photograph 38-081 was omitted because of redundancy). The shuttle photographs reveal few clouds. Since the surface of the ocean is not smooth, the sun is not reflected back to the shuttle as a disc but as a distorted, vague-edged image, whose distortion is determined by the amount of surface roughness and the solar incident angle. In each of the photographs, the sun's reflection on the ocean surface is shown, with its position determined by the angle of the sun and the spacecraft in relation to the ocean surface. As the shuttle moves, the angle changes and the reflection moves. Thus, as the shuttle sweeps over the ocean, the reflection moves as if a spotlight were illuminating the vast interconnection of ocean features. In this mosaic, stress lines related to the shear of the currents are prominently defined. Also seen are anticyclonic spiral eddies associated with the front. (The prominent east–west lines are ship tracks.)

(b) A NOAA AVHRR-IR image, taken approximately 3 hours after the shuttle's passage, gives the geographic location of the mosaic. Because it is difficult to mark the mosaic without interfering with the visual details of the photographs, the reader is asked to compare by eye the infrared image and the mosaic and to note the many similarities between the thermal features and the frontal features, including the lines of shear and eddy fields. (NOAA satellite data collected by Royal Aircraft Establishment, Farnborough, England.)

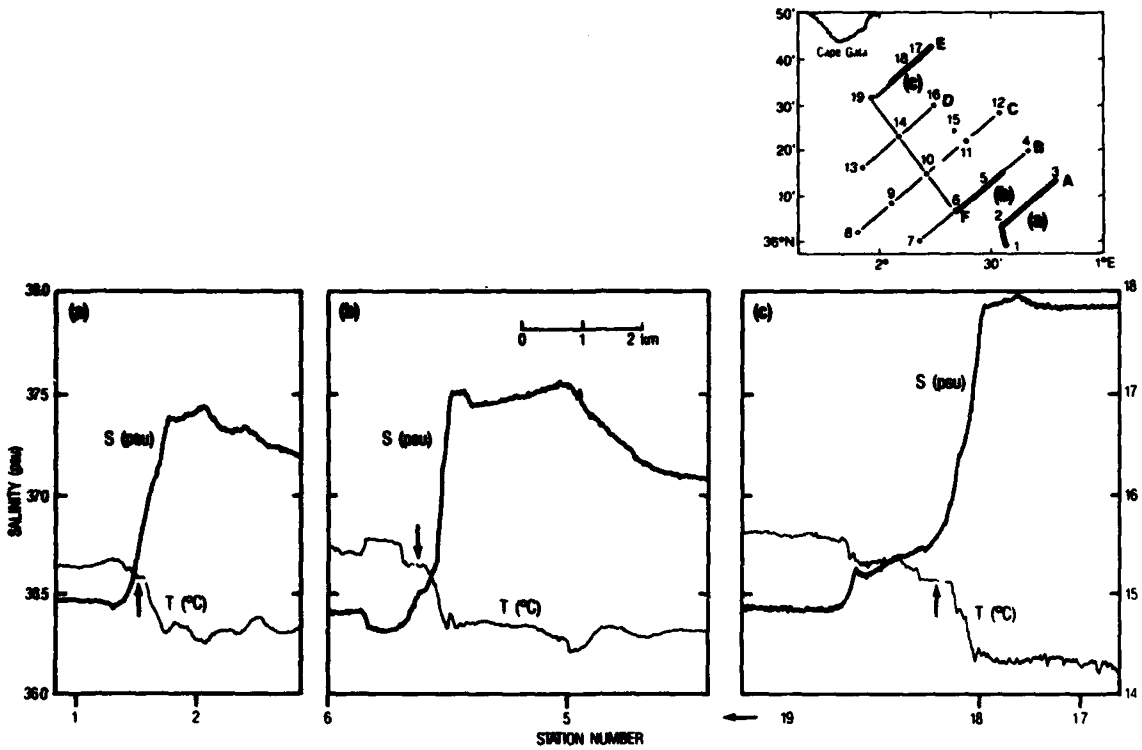


FIG. 5. Thermosalinograph data across the front for portions of Sections A, B and E: (a) Stations 1, 2 and 3; (b) Stations 4, 5, 6 and 7; and (c) Stations 17, 18 and 19.

sumed 36 hours later at the same position. A comparison of XBTs dropped at the same position before and after the gale shows that a cooling of the surface mixed layer (30 m) was the only appreciable change that occurred during the 36 hours. We have therefore assumed synopticity for data below this layer.

### b. Observations and results

Figure 4b shows the relation of the ship's track to the surface thermal manifestation of the front, which is indicated by the only clear-sky NOAA infrared image available for the survey period. The front was also visible from the deck of the ship, and the color change across the front was quite marked. Although calm farther away from the color change, the sea surface at the discontinuity included breaking waves, foam, an accumulation of detrital material and many feeding birds. The "sea clutter" in the ship's radar also defined the region of the front in a manner similar to the aircraft radar in section 2. Most important, the front was detected at depth in each of the several sectional analyses of the data, indicating that the surface color and roughness phenomena noted during the cruise and in the aircraft/shuttle study were related to subsurface oceanographic processes.

#### 1) SURFACE STRUCTURE

The surface thermosalinograph data (Fig. 5) show two things: first, that the strong gradients of the two parameters associated with the front coincide, thus giving credence to the use of thermal satellite imagery to monitor the front; and second, that the temperature and salinity gradients are much stronger than would be indicated by the station data alone (the thermosalinograph showed that the surface changes had occurred over a distance of less than 4 km, although a distance of 10 km was normal). The horizontal gradient observed in the northernmost crossing (between Stations 17 and 19) showed the strongest changes, with salinity varying between 36.41 and 37.99 psu and temperature between 15.8° and 14.4°C (Fig. 5c).

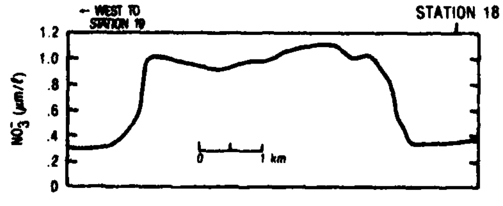


FIG. 6. Surface nitrates between Stations 18 and 19.

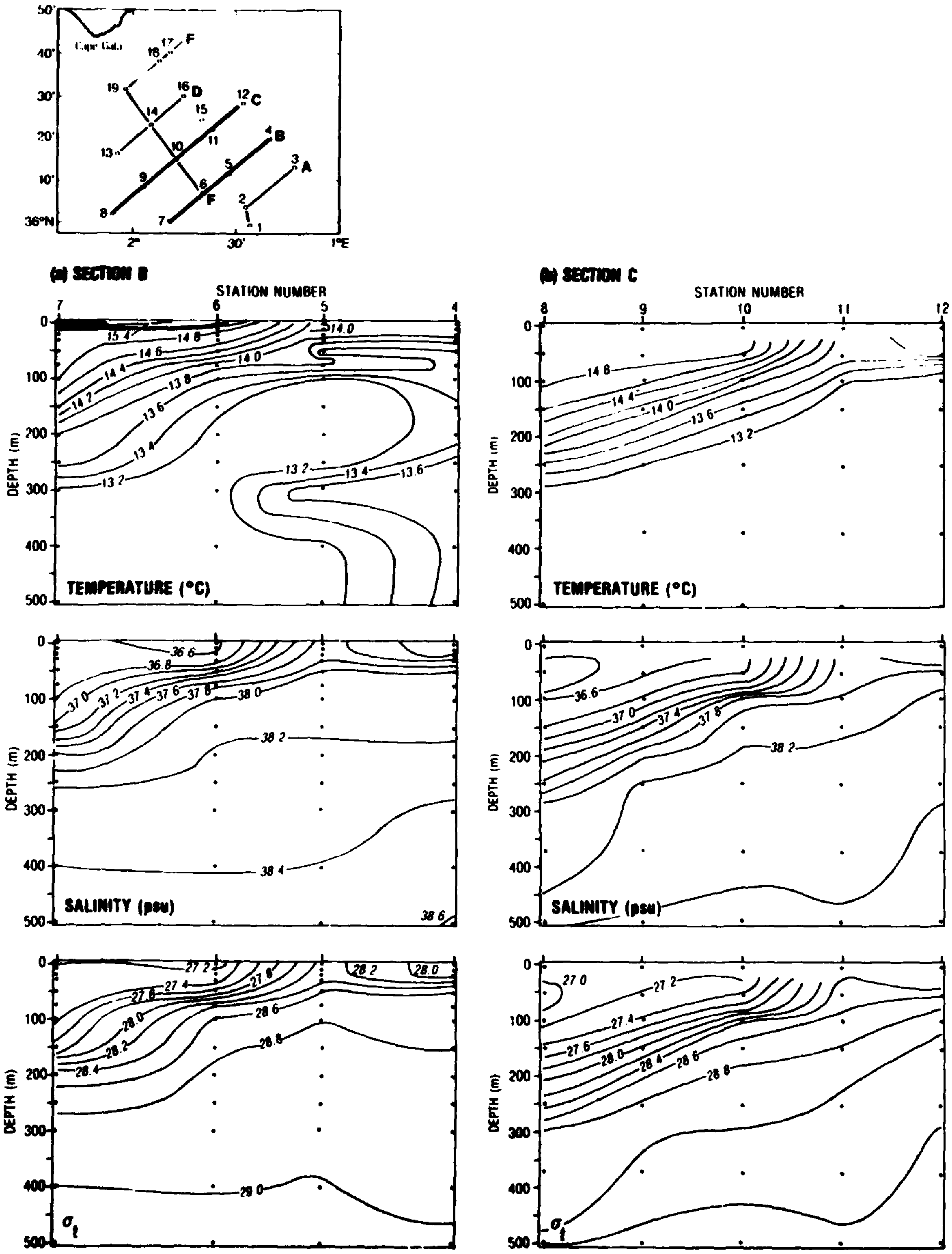


FIG. 7. Vertical temperature, salinity, and density distribution for (a) Section B and (b) Section C.

The surface data also revealed another factor. The arrows in Fig. 5 point to a zone of uniform surface temperature just west of the sharp salinity/temperature change, which suggests intense upward motion or mixing. This zone, which appeared on the western side of the front in all sections, was approximately 1 km wide for the first two crossings and wider (about 2 km) in the northern sections. Surface nitrate levels were generally higher on the western side of the front, apparently in conjunction with this region of uniform temperature. Although low (0.2–0.3 $\mu$mol l$^{-1}$) immediately at the front (Station 18), surface nitrate values increased 2 km west of the front and reached a maximum of slightly more than 1 $\mu$mol l$^{-1}$ at 3 km. The width of the maximum surface nitrate area was approximately 7 km (Fig. 6).

### 2) Cross-front structure

The vertical structure of the density front is well demonstrated for Sections B and C in Figs. 7a and 7b. At the surface, an intrusion of warm MAW can be observed in the upper 10 m between Stations 7 and 6 of Section B. At depth in both Sections B and C, temperature, salinity and density isolines generally tilt upward toward the east, indicating strong vertical movement.

Figures 8a and 8b show the vertical nitrate/nitrite distribution across the front along Sections B and C (for emphasis, the 28.4 isopycnal has been added as a dashed line in the figure). Along Section B, very low concentrations were observed in the surface layer near the front (Station 5), and at 75 and 200 m to the east of the front (Stations 6 and 7). Figure 9 uses nitrate/sigma-*t* coordinates to show that these relative minima lie over the same isopycnal surface: 28.4.

The oxygen and nitrogen data can be used as tracers of the subsurface circulation. Figures 8b and 8c indicate that oxygen and nitrate/nitrites followed similar patterns in the sigma-*t* field, and that the relative oxygen maximum also coincided with the 28.4 isopycnal (oxygen sampling was not done at all stations along Section B; thus no oxygen section is presented). The existence of the nitrate minima and oxygen maxima at different depths but on the same isopycnal surface suggests an along-isopycnal displacement, or sinking, of water that had originally been at the surface. This along-isopycnal flow appears to have occurred along both Sections B and C (although the deeper movement along Section C may possibly be due to the distortion of the surface layer by the 36-hour period of high winds).

The onboard echosounder (38 kHz) presents further evidence of this type of circulation. For example, along Section E, it clearly registered a distortion of the scattering layer across the front between Stations 17 and 19 (Fig. 10). At the surface front (Station 18), an intense signal was detected, while westward (i.e., toward Station 19), this signal weakened and a layered structure was observed. Higher signal echo and intensity were found along tilted surfaces whose intersection with the surface coincided with the increase of surface nitrate concentrations. The slope of both the echosounder lines and the isopycnal surfaces between Stations 18 and 19 was

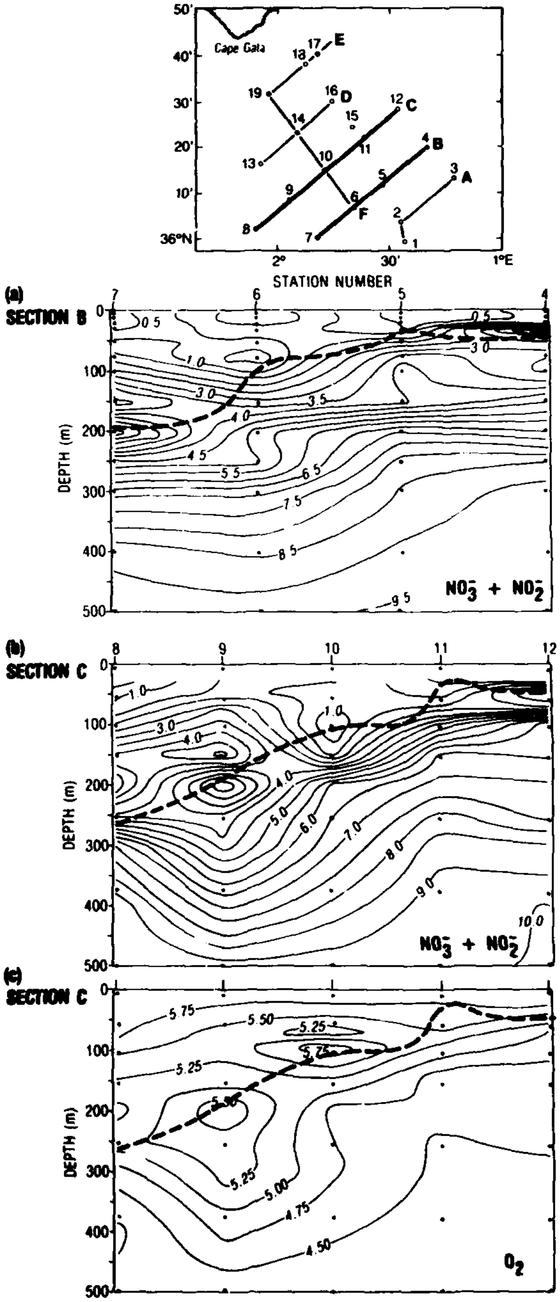


FIG. 8. Vertical nitrogen distribution for (a) Section B, and (b) Section C. Vertical oxygen distribution for Section C (c). The dashed line represents the depth of the 28.4 isopycnal.

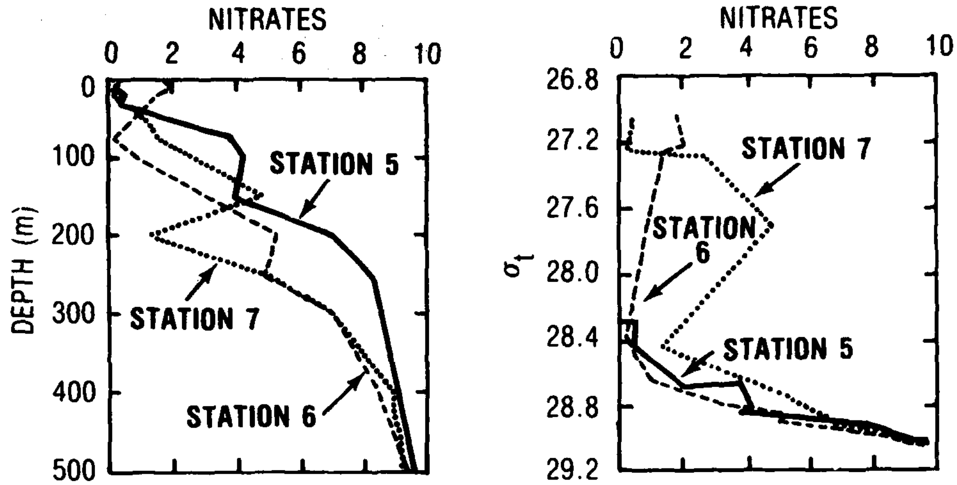


FIG. 9. Vertical nitrogen versus depth (a) and sigma-$t$ (b) for section B.

estimated to be the same—0.009—suggesting that the targets were also distributed along isopycnals.

The biological data also indicate strong vertical and horizontal movement near the front. The vertical chlorophyll distribution along Section B, for example, indicates that strong vertical motion or mixing was taking place in the upper 50 m below the surface position of the front (Fig. 11).

### 3) Along-front structure

A striking along-front uniformity was observed, with a strong vertical gradient between 50 and 100 m (Sec-

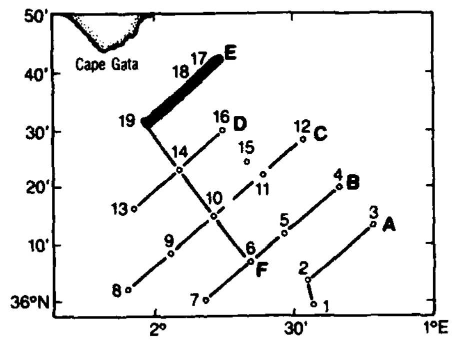


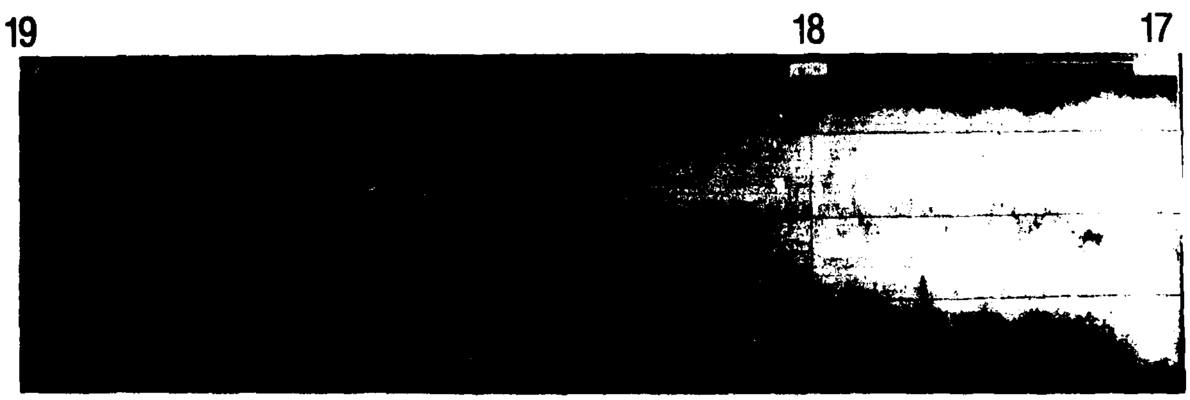


FIG. 10. Echosounder chart for Section E.

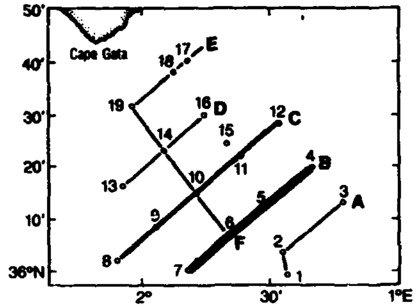


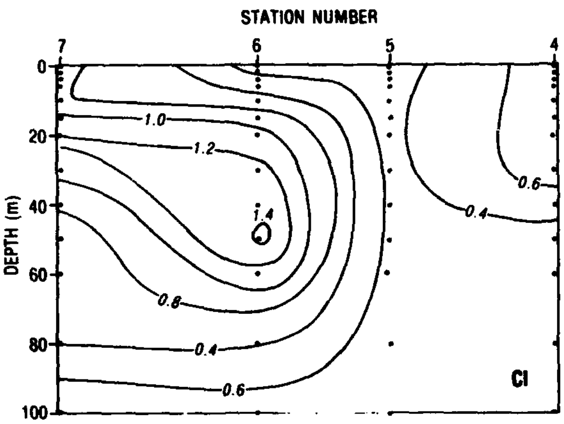


FIG. 11. Vertical chlorophyll distribution for Section B.

tion F, Fig. 12a). Figure 12b shows the horizontal variation in depth of the 28.2 isopycnal surface, and in effect, demonstrates the variation in depth of the nitrate minima and oxygen maxima (see Figs. 8 and 9). Horizontal cuts at different levels also show the nitrate/pycnal relationship (Figs. 13a, b). At 30 m, very low nitrate concentrations (lower than 0.3 $\mu$mol $l^{-1}$) were detected at Stations 12, 16 and 18, while relative nitrate maxima were found at 75 m at Stations 19 and 14.

## 4. Discussion

The Almeria–Oran front is a large-scale density front (Ro = 0.3) formed by the convergence of two very distinct water masses. The circulation associated with a surface buoyant inflow was studied by Kao et al. (1977) and the mutual intrusion of a gravity current was investigated by Wang (1984). According to these numerical studies, a stationary front in quasi-geostrophic balance is achieved. We have therefore investigated the along-front circulation and horizontal shear and have computed geostrophic along-front currents taking the reference level at 400 m. This level is meaningful, since the LIW is found between 200 and 600 m and propagates southwestward at around 1 cm $s^{-1}$ (Parrilla and Kinder 1987). The surface dynamic height indicates a surface jet of approximately 100 cm $s^{-1}$ centered between Stations 6 and 7 (Fig. 14). In Fig. 13, Section B shows a strong horizontal shear in the cross-front direction and high currents in the upper 50 m west of the surface front. The current is surface-intensified and stronger on the western side of the front.

In the southern region, two cyclonic eddies are observed, with denser waters found east of lighter waters (Fig. 13a). At 75 m, Fig. 13b shows that the expected density distribution with denser water on the eastern side was already present (the instability observed in the surface sigma-$t$ field appears as a meander at 75 m). The length scale of this instability is about 20 km, which is similar to the baroclinic Rossby radius $LD = 20$ km (with $N = 6 \times 10$ $s^{-1}$ and $H = 300$ m).

No current meters were used during the ship study, so we cannot compare these computed values with actual current measurements. However, a rough estimate, based on the ship's drift in calm seas and a 3 m $s^{-1}$ wind from Station 15 to 16 (very close to the surface front) and using two very close satellite fixes (69 minutes apart), indicated a surface current of 1 m $s^{-1}$ toward the south-southwest (200°T). This value is similar to the computed geostrophic current, and the current direction indicates a strong ageostrophic cross-frontal circulation.

The appearance of the strong surface convergence at the front indicates that intense vertical motions must have been taking place. In order to study the subsurface features in relation to the observed surface convergence, Station 18 was deliberately positioned directly over the surface discontinuity. At this station, a low surface concentration of nitrate was found. The sudden increase in nitrate concentration detected west of the station (Fig. 6) coincides with the beginning of the zone of uniform surface temperature (Fig. 5) and the intersection of the echosounder lines with the sea surface (Fig. 10). Similar features characteristic of upwelling were found at Section B, with high nutrient and low oxygen concentrations at Station 6 (20 km west of the surface front), and low nutrient and high oxygen concentrations at Station 5 (3.5 km east of the surface front).

As in most organic density fronts, higher biological activity was observed (Fig. 10). The higher biological activity often found in frontal regions (Savidge 1976; Houghton and Marra 1983) is believed to be associated with the cross-frontal circulation induced by nonlinear and friction forces (James 1978; Simpson and James 1986). However, the existence of a complex "multi-cell" circulation (Mooers et al. 1978) associated with density fronts has long been a controversial subject (Brink 1987). In our case, the cross-frontal circulation presented an along-isopycnal sinking associated with the surface convergence east of the front and an upwelling in the less dense waters west of the surface front. The width of the upwelling region, estimated from Fig.

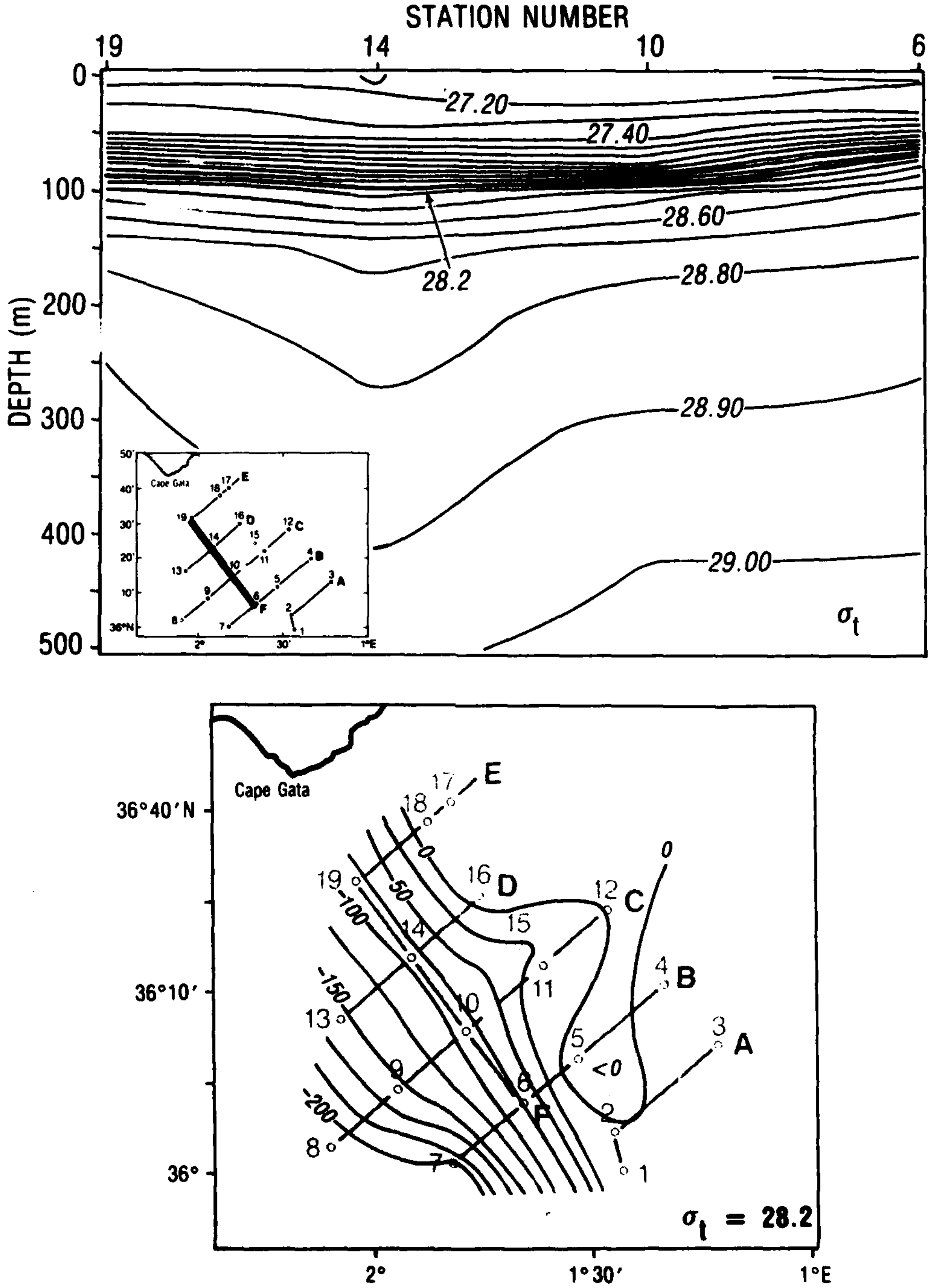


FIG. 12. (a) Along-front distribution of density (sigma-$t$) for Section F. (b) Depth of 28.2 isopycnal.

6, is approximately 7 km. This secondary circulation pattern agrees qualitatively with previous numerical studies in a frontal region (Kao et al. 1978; Wang 1984; James 1984).

## 5. Conclusions

Our analysis of physical, chemical and biological data from the R/V *Garcia del Cid* field study combined with satellite imagery, shuttle photographs, and aircraft

XBT data shows that the Almeria–Oran Front is a sharp density front limited to the upper 300 m, with a strong baroclinic jet in the upper 50 to 75 m. The front appears to be controlled by the size and position of the Eastern Alboran Sea Gyre. As a result, a strong flow of Atlantic-derived waters is contained near the Spanish coast to a point south of Cape Gata. From this point the water is deflected southeastward toward the African coast, where part returns westward still entrained in the Eastern Alboran Gyre, and an apparently larger part continues eastward along the African coast. East of Cape Gata, southward-flowing MW converges with the AW to form the well-defined, large-scale frontal zone we call the Almeria–Oran Front. The secondary circulation is characterized by surface convergence, along-isopycnal sinking, and upwelling west of the surface front.

The initial investigation of the region was conducted as part of a one-year WMCE field program. More studies of the Almeria–Oran Front will be published as the data from these field efforts are analyzed.

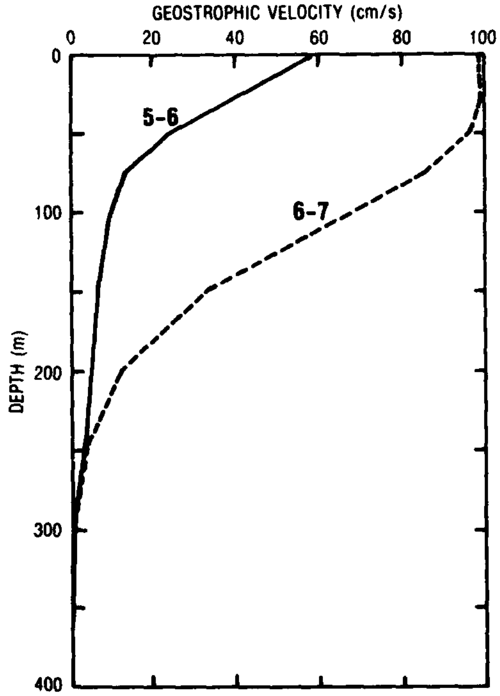


FIG. 14. Geostrophic profiles between Stations 6 and 7 and Stations 5 and 6. Dynamic heights were computed from the hydrographic data, assuming a reference height of 400 m rather than 500 m because several Nisken bottles did not close at the 500 m depth.

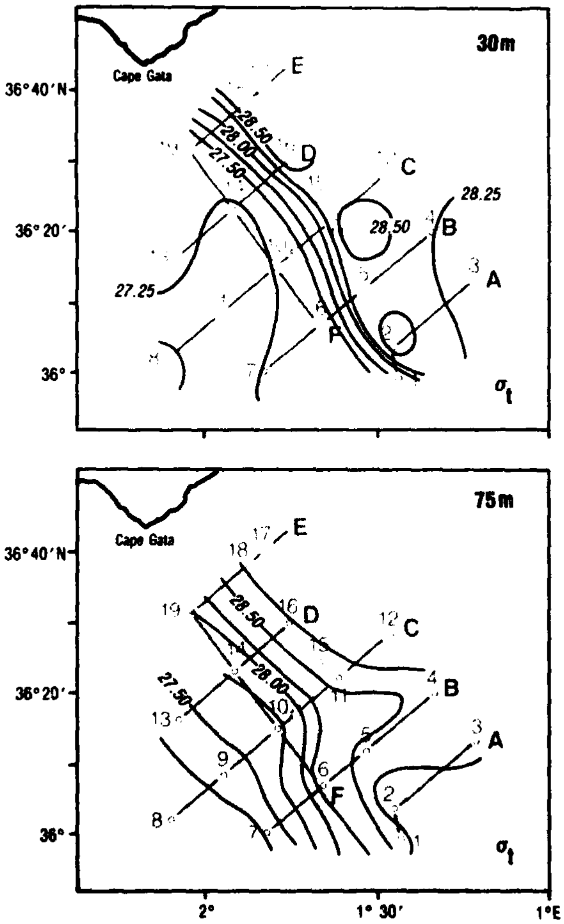


FIG. 13. (a) Distribution of density (sigma-*t*) at 30 m and (b) 75 m.

*Acknowledgments.* Agusti Julia provided technical assistance, and Jordi Font and Mario Manriquez helped with the processing of the data. Robert Arnone helped with the collection of the aircraft data during the presurvey studies. In this regard, exceptional thanks should go to the crew of space shuttle mission STS-41-G for their cooperation in taking photographs of the front. Useful discussions with Dong Ping Wang, Robert Arnone and Denis Wiesenburg increased the quality of the manuscript and are gratefully acknowledged. J. Tintore and I. Blade were sponsored by the Spanish "Ministerio de Educacion y Ciencia" through a Doctoral Fellowship. P. E. La Violette was sponsored by the Director of the U.S. Office of Naval Research, NORDA Contribution 321:047:87.

## REFERENCES

Arnone, R. A., and P. E. La Violette, 1984: Bio-optical variability in the Alboran Sea as assessed by Nimbus-7 Coastal Zone Color Scanner. NORDA Tech. Note 283, 29 pp.

——, D. A. Wiesenburg and K. D. Saunders, 1987: Origins and characteristics of the Algerian Current. *Eos, Trans. Amer. Geophys. Union*, 68(50), p. 1725.

Arnone, 1988.

Brink, K. H., 1987: Coastal ocean physical processes. *Rev. Geophys. Space Phys.* **25**(2), 204–216.

Bryden, H. L., and T. H. Kinder, 1986: Gibraltar experiment: A plan for dynamic and kinematic investigations of strait mixing, exchange and turbulence. WHOI Rep. WHOI-86-29, 82 p.

Carpenter, J. H., 1965: The accuracy of the Winkler method for dissolved oxygen analysis. *Limnol. Oceanogr.*, **10**, 135–140.

Cheney, R. E., 1977: Aerial observations of oceanic fronts in the western Mediterranean Sea. U.S. Naval Oceanographic Office Tech. Note 3700-69-77, 23 pp.

Donde Va? Group, Donde Va?, 1984: An oceanographic experiment in the Alboran Sea. *Eos, Trans. Amer. Geophys. Union*, **65**(36), 682–683.

Gascard, C., and C. Richez, 1985: Water masses and circulation in the western Alboran Sea and in the Strait of Gibraltar. *Progress in Oceanography*, Vol. 15, Pergamon, 152–216.

Heburn, G., and P. E. La Violette, 1987: Related variations in the structure of the anticyclonic gyres found in the Alboran Sea. *Eos, Trans. Amer. Geophys. Union*, **68**(50), 1725.

Houghton, R. W., and J. Marra, 1983: Physical biological structure and exchange across the thermohaline shelf slope front in the New York Bight. *J. Geophys. Res.*, **88**(C7), 4467–4481.

James, I. D., 1978: A note on the circulation induced by shallow sea fronts. *Estuar. Coastal Mar. Sci.*, 7, 197–202.

——, 1984: A three dimensional numerical shelf-sea front model with variable eddy viscosity and diffusivity. *Contin. Shelf Res.*, 3(1), 69–98.

Jeffrey, S. W., and G. F. Humphrey, 1972: New spectrophotometric equations for determining chlorophylls a, b, c, and C in higher plants, algae and natural phytoplankton. *Biochem. Physiol. Pflanz*, **167**, 191–194.

Kao, T. W., H-P. Pao and C. Park, 1978: Surface intrusions, fronts and internal waves: A numerical study. *J. Geophys. Res.*, **83**, 4641–4650.

Lacombe, H., and P. Tchernia, 1972: Caractères hydrologiques et circulation des eaux en Mediterranée. *The Mediterranean Sea*, D. J. Stanley, Ed., Dowden, Hutchinson, and Ross, 26–36.

Lanoix, F., 1974: Project Alboran: Étude hydrologique et dynamique de la Mer d'Alboran. NATO Tech. Rep. 66, p. 36; 32 figs.

La Violette, P. E., 1984: The advection of submesoscale thermal features in the Alboran Sea Gyre. *J. Phys. Oceanogr.*, **14**, 550–565.

——, 1987: Portion of Western Mediterranean Circulation Experiment completed. *Eos, Trans. Amer. Geophys. Union*, **68**(9), 123–124.

Mooers, C. N. K., C. A. Collins and R. L. Smith, 1978: The dynamic structure of the frontal zone in the coastal upwelling region off Oregon. *J. Phys. Oceanogr.*, **6**, 3–21.

Parrilla, G., and T. H. Kinder, 1987: The physical oceanography of the Alboran Sea. NORDA Rep. 184, 26 p.

——, —— and R. H. Preller, 1986: Deep and intermediate water in the western Alboran Sea. *Deep-Sea Res.*, 33, 55–88.

Perkins, H., T. H. Kinder and P. E. La Violette, 1987: Variation in the Alboran Sea Gyre and its relationship to meteorological forcing in the Gulf of Cadiz. *Eos, Trans. Amer. Geophys. Union*, **68**(50), 1725.

Phillipe, M., and L. Harang, 1982: A reduced gravity model of circulation in the Alboran Sea. *Hydrodynamics of Semi-Enclosed Seas*, J. C. J. Nihoul, Ed., Elsevier, 91–128.

Preller, R., and H. E. Hurlburt, 1982: A reduced gravity model of circulation in the Alboran Sea. *Hydrodynamics of Semi-Enclosed Seas*, J. C. J. Nihoul, Ed., Elsevier, 75–90.

Savidge, G., 1976: A preliminary study of the distribution of chlorophyll in the vicinity of fronts in the Celtic and western Irish Seas. *Estuar. Coastal Mar. Sci.* **4**, 617–625.

Simpson, J. H., and I. D. James, 1986: Coastal and estuarine fronts. *Baroclinic Processes on Continental Shelves*, C. N. K. Mooers, Ed., AGU.

Strickland, J. D., and T. R. Parsons, 1972: A practical handbook of seawater analyses. *J. Fish. Res. Bd. Canada*, **167**, 1–310.

Wang, D. P., 1984: Mutual intrusions of a current and density front formation. *J. Phys. Oceanogr.*, 7, 1191–1199.

Werner, F., A. Cantos and G. Parrilla, A sensitivity study of reduced gravity channel flow with application to the Alboran Sea. *J. Phys. Oceanogr.*, in press.